Analecta Technica Szegedinensia
Vol. 16, No. 01 ISSN 2064-7964 2022

EVALUATION OF GEAR PITTING SEVERITY BY USING VARIOUS CONDITION MONITORING INDICATORS

[1]Camelia R. Sfetcu, [1]Zoltan I. Korka, [1]Alin V. Bloju, [1]Dalina E. Traistaru, [1]Corneliu Hrimiuc*

[1] Babeş-Bolyai University, Doctoral School of Engineering, P-ta Traian Vuia no. 1-4, 320085 Resita, Romania
*e-mail: zoltan.korka@ubbcluj.ro

ABSTRACT

Fault detection techniques based on vibration measurement are implemented to identify in an early stage failures appearing in gear transmissions. Condition monitoring indicators (CMI), like: Root Mean Square (RMS), Crest Factor, Kurtosis, FMO, FM4, Energy ratio, Energy operator, NA4 or NB4, are used to estimate the level of gear faults such as pitting, cracks, spalling, scuffing or scoring. However, in is multitude of indicators, the question that arises is: which CMI is the most sensitive in estimating the severity of defects? Thus, this paper presents an extensive comparison between the before mentioned indicators computed from vibration signals collected on four pinions with different pitting grades, created by artificial means. The pinions where incorporated in a single helical gearbox and the tests were performed on an open-energy test rig at three different input speeds. This comparative study assesses the receptivity of different condition monitoring indicators towards gear pitting failure. We concluded that all the involved indicators are responsive and sensitive to fault diagnosis, even in low speed operating conditions.

Keywords: condition monitoring indicators, fault diagnosis, gear pitting

1. INTRODUCTION

Gearboxes are widely used in different industrial applications, because, compared to other mechanical transmissions, they are capable to transmit, both speeds and high moments, in small volumes. When the gear teeth are loaded near to their maximum capacity, they are forced to endure high contact pressures, which are leading to various fatigue deteriorations, such as scoring, scuffing, spalling or pitting. These failures occur even under proper lubrication conditions of the gears and represent nearly 60% of the damages in the gearboxes components [1].

Pitting is the most common failure of the gear teeth surface, working under oil lubrication conditions [2], [3]. It is initiated in the inclusions from the gear material, which act as stress concentrators, spreading parallel and below the teeth surfaces. When these cracks are joining or are breaking through the tooth surface, material separation occurs forming the so-called pits.

In the last decades were developed different gear fault diagnosis methods and condition monitoring techniques [4], [5], [6]. Fundamentally, vibration signals acquired from gearboxes by means of accelerometers, are filtered, amplified, processed and analysed in time domain [7], frequency domain [8], or time-frequency domain [9].

With the fast development of artificial intelligence technologies, classification of gear faults using machine learning became a hot topic in the field of gear fault diagnosis methods. Thus, Liu et al. [10] proposed a personalized fault diagnosis method using finite element method simulation and extreme learning machine to detect faults in gears. Further, He et al. [11] introduce a deep transfer multi-wavelet auto-encoder for intelligent gear fault diagnosis with small training samples.

Statistical indicators, likewise known as condition monitoring indicators, are also extensively used to identify failures in gear transmissions appearing in an early stage [12]. However, in the bunch of indicators, the doubt that rises is: which of these CMI's is the most sensitive, being able to assess the gear fault severity. Therefore, this paper aims to analyse the responsiveness of different indicators towards gear pitting severity. Incorporating four pinions with various pitting grades, made by artificial means, in a single helical gearbox, vibration measurements were performed at three different input speeds, on an open-energy

DOI: https://doi.org/10.14232/analecta.2022.1.34-41

test rig. Finally, the research has concluded regarding the receptivity of the involved condition monitoring indicators to predict gear-pitting severity.

2. CONDITION MONITORING INDICATORS

Following CMI's were involved in the present research:

2.1. Root Mean Square

The root mean square (RMS) of a continuous-time waveform is the square root of the arithmetic mean of the squares of the values, or the square of the function that defines the continuous waveform. RMS was initially developed to characterize the heating of a resistor exposed to a sine wave varying current. In case of a set of *n* values $\{x_1, x_2, \ldots, x_n\}$ the RMS is:

$$RMS_x = \left(\frac{1}{n}\sum_{i=1}^{n} x_i^2\right)^{0.5} \tag{1}$$

2.2. Crest Factor

The Crest Factor (CF) is a parameter of a waveform showing the ratio of the maximum positive peak value to the RMS value:

$$CF = \frac{\max(x_1, x_2, \ldots, x_n)}{RMS_x} \tag{2}$$

Crest factor is a normalized parameter of the signal amplitude. A signal with a few high amplitude peaks are producing a bigger CF, as the numerator increases (high amplitude peaks), while the denominator decreases (few peaks means lower RMS).

2.3. Kurtosis

The shape of the amplitude disposal is regularly involved as a data descriptor. Kurtosis shows how peaked or flat a waveform signal is. When a vibration signal incorporates sharp peaks with higher value, then the distribution function will be sharper. We can presume that damaged gears produce these types of waves. Consequently, a damaged gear will have higher kurtosis value then a healthy gear. A mathematical expression of Kurtosis is given in (3):

$$K = \frac{n \cdot \sum_{i=1}^{n}(x_i - \bar{x})^4}{(\sum_{i=1}^{n}(x_i - \bar{x})^2)^2} \tag{3}$$

where $\bar{x}$ is the mean value of the signal.

2.4. Zero-order Figure of Merit (FM0)

The zero-order figure of merit (FM0) is an indicator of major faults in a gear mesh, being defined as the ratio between the peak-to-peak value of a signal and the energy of the mesh frequency and its harmonics. In contrast to CF, which compares the peak value of the synchronous averaged signal with the energy of the synchronous averaged signal, FMO compares the same peak value of the synchronous averaged signal, with the energy of the regular signal. Thus, FMO is deducted as:

DOI: https://doi.org/10.14232/analecta.2022.1.34-41

$$FM0 = \frac{x_{max} - x_{min}}{\sum_{i=1}^{n} A(i)} \tag{4}$$

where x_{max} is the maximum amplitude of the signal, x_{min} the minimum amplitude of the signal, *A(i)* is the amplitude of the *i-th* mesh frequency harmonics and *n* is the total number of harmonics in the frequency spectrum.

2.5. Fourth-order Figure of Merit FM4

Fourth-order figure of merit (FM4) was designed to improveFM0 in the detection of damages located only on a finite number of gear teeth. This can be done by removing the gear meshing frequency and its harmonics from the time synchronous average signal. The obtained result is the so-called differential signal *d*. FM4 is computed as:

$$FM4 = \frac{n \cdot \sum_{i=1}^{n} \left(d_i - \bar{d}\right)^4}{\left(\sum_{i=1}^{n} \left(d_i - \bar{d}\right)^2\right)^2} \tag{5}$$

where $\bar{d}$ is the mean of the differential signal, d_i the *i*-th point of the differential signal the time signal and *N* the total number of data points in the time signal.

2.6. Energy Ratio (ER)

Energy ratio (ER) is an indicator for uniform wear. It is computed as the ratio of the RMS of the difference signal *d* to the RMS of the signal containing only the regular meshing components x_d:

$$ER = \frac{RMS_d}{RMS_{x_d}} \tag{6}$$

As wear progresses, energy moves from the regular signal to the difference signal.

2.7. Energy Operator (EOP)

Is calculated as a normalized kurtosis of a so-called resultant signal (*re*), *re* being computed as a difference between the squared input signal for each point x_i ($i=1....n$) and the product of the point before and after ($x_{i-1} \cdot x_{i+1}$):

$$EOP = \frac{n \cdot \sum_{i=1}^{n} (re_i - \overline{re})^4}{\left(\sum_{i=1}^{n} (re_i - \overline{re})^2\right)^2}, \tag{7}$$

where $re_i = x_i^2 - x_{i-1} \cdot x_{i+1}$ is the i[th] measurement of the resulting signal *re* and $\overline{re}$ is the average of the resulting signal. In case of the endpoints, the signal is assumed to be a continuous loop, meaning that for calculating the first point is involved the last point and inversely.

2.8. NA4

The NA4 parameter was evolved to overcome the deficiency of FM4, which becomes less sensitive as the manifestation of faults grows in both number and severity. Two changes were done to develop NA4 to be more sensitive to the damage evolution: firstly, it is computed from the residual signal and secondly, trending was incorporated into the parameter. Thus, NA4 is calculated as the ratio of fourth moment of the residual signal to the square of its run time averaged variance:

DOI: https://doi.org/10.14232/analecta.2022.1.34-41

$$NA4 = \frac{n \cdot \sum_{i=1}^{n} \left(r_{i_M} - \overline{r_M}\right)^4}{\left\{\frac{1}{m}\sum_{j=1}^{m}\left[\sum_{i=1}^{n}\left(r_{ij} - \bar{r}_j\right)^2\right]\right\}^2}\ , \tag{8}$$

where $\bar{r}$ is the mean of the residual signal, *n* the total number of data points in the time signal, *j* the index of the time signal in the run ensemble, and *m* the number of the current time signal.

2.9. NB4

NB4 is computed as a time-averaged kurtosis of the envelope of the signal after it was band-pass filtered about the mesh frequency. The envelope *s(t)* is calculated involving the Hilbert Transform, being given by:

$$s(t) = |\{b(t) + iH[b(t)]\}|\ , \tag{9}$$

where, *b(t)* is band-pass filtered signal about the mesh frequency, *i* the number of samples and $H[b(t)]$ the Hilbert Transform of *b(t)*.

3. MATERIALS AND METHODS

For the evaluation of the gear pitting by involving the upper described CMI's, an open-energy test stand was used. The main components of the stand are shown in Fig. 1, these being: an electric motor with variable speed, the gearbox and a hydraulic pump, used as a brake.

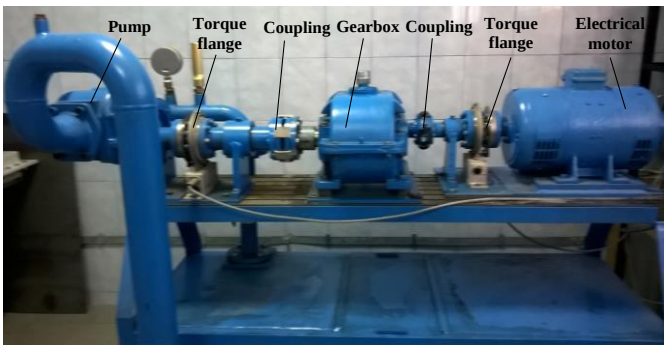

Figure 1. Main components of the test stand [13]

The connection between these components was made through two couplings with rubber strips, which ensure a good torsional vibration damping and allow a smooth assembling. For reading the input speed and the torques on the input shaft and output shaft respectively, two torque flanges of type T 10 FE, made by HBM- Germany, were used.

Table 1. Technical data of the test stand

Element	*Technical data*	
Electric motor	Power:	P_{max}= 2,5 kW
	Speed:	n= 0…1500 min^{-1}
Gearbox	Centre distance:	A= 125 mm
	Teeth number:	z_1/ z_2= 17/ 43
	Module	m_n= 4 mm
	Face width	b= 40 mm
	Helix angle	β= 11°
Break	KF 6/400 gear pump (KRACHT)	

DOI: https://doi.org/10.14232/analecta.2022.1.34-41

A Kistler made accelerometer of type 8772, placed on the top of the gearbox housing, above the high-speed shaft, was used for vibration measurements. The vibration signals were acquired via a 92234 National Instruments module, placed in a chassis cDAQ-9172.
For fine processing, the vibration signals were sent to a laptop programmed to run in LabView software a self-developed application. The main technical data of the test stand are described in Tab. 1.
The before mentioned CMI's were computed from vibration signals collected on four pinions with different pitting conditions, created by practicing artificial grooves with a diameter of 3 mm and a depth of about 0.5 mm, along the pitch line of the teeth. The pinions with different failure status (PC1- healthy teeth; PC2- teeth with slight pitting; PC3- teeth with mild pitting; PC4- teeth with acute pitting) are presented in Fig. 2.

PC1 PC2 PC3 PC4

Figure 2. Pinions with different failure status

The experimental procedure was conducted following the below mentioned steps:
- the healthy pinion (PC1- status) was assembled into the gearbox and the test stand was operated in turn, at following input speeds: 1000, 1250 and 1500 min^{-1};
- collection, storage and processing of the vibration signals;
- replacement of the pinion with PC1- status with the one having PC2- status, followed by the resumption of steps described above;
- continuation of experimental measurements, as before described, for the other two pinions.

4. RESULTS AND DISCUSSION

CMI's for pinions with different failure status operating at three different speeds have been evaluated. Values of the nine parameters described in Section 2 were computed, being organized in Tab. 2. To have a better image about how the nine condition parameters are influenced by the input speed of the gearbox and the pitting severity, Fig. 3 depicts the variation of the CMI's for the three operating speeds and the four pinion healthy conditions.

Table 2. Condition Monitoring Indicators

CMI	n_1= 1000 min^{-1}				n_1= 1250 min^{-1}				n_1= 1500 min^{-1}			
	PC1	PC2	PC3	PC4	PC1	PC2	PC3	PC4	PC1	PC2	PC3	PC4
RMS	1,005	1,234	1,896	2,314	1,055	1,750	2,514	3,088	1,075	2,254	3,756	6,988
CF	2,755	2,890	3,550	4,215	2,815	3,025	3,770	4,890	2,865	4,326	5,132	6,309
K	3,021	3,775	3,895	4,777	3,210	3,995	5,210	6,455	3,431	4,055	6,643	9,342
FM0	0,008	0,009	0,011	0,010	0,008	0,010	0,012	0,013	0,010	0,003	0,015	0,022
FM4	2,890	3,150	3,364	3,955	3,050	3,390	3,675	4,750	3,179	4,305	5,925	7,795
ER	0,555	0,690	0,712	0,798	0,595	0,722	0,756	0,912	0,605	1,765	2,095	2,849
EOP	2,987	7,855	10,025	11,250	3,025	5,677	8,875	15,554	3,519	11,207	19,764	38,733
NA4	3,015	3,187	3,247	3,998	3,010	3,022	3,225	4,205	3,035	4,115	4,435	4,878
NB4	2,225	2,220	2,415	3,895	2,195	2,945	4,895	6,473	2,218	4,068	6,218	10,764

DOI: https://doi.org/10.14232/analecta.2022.1.34-41

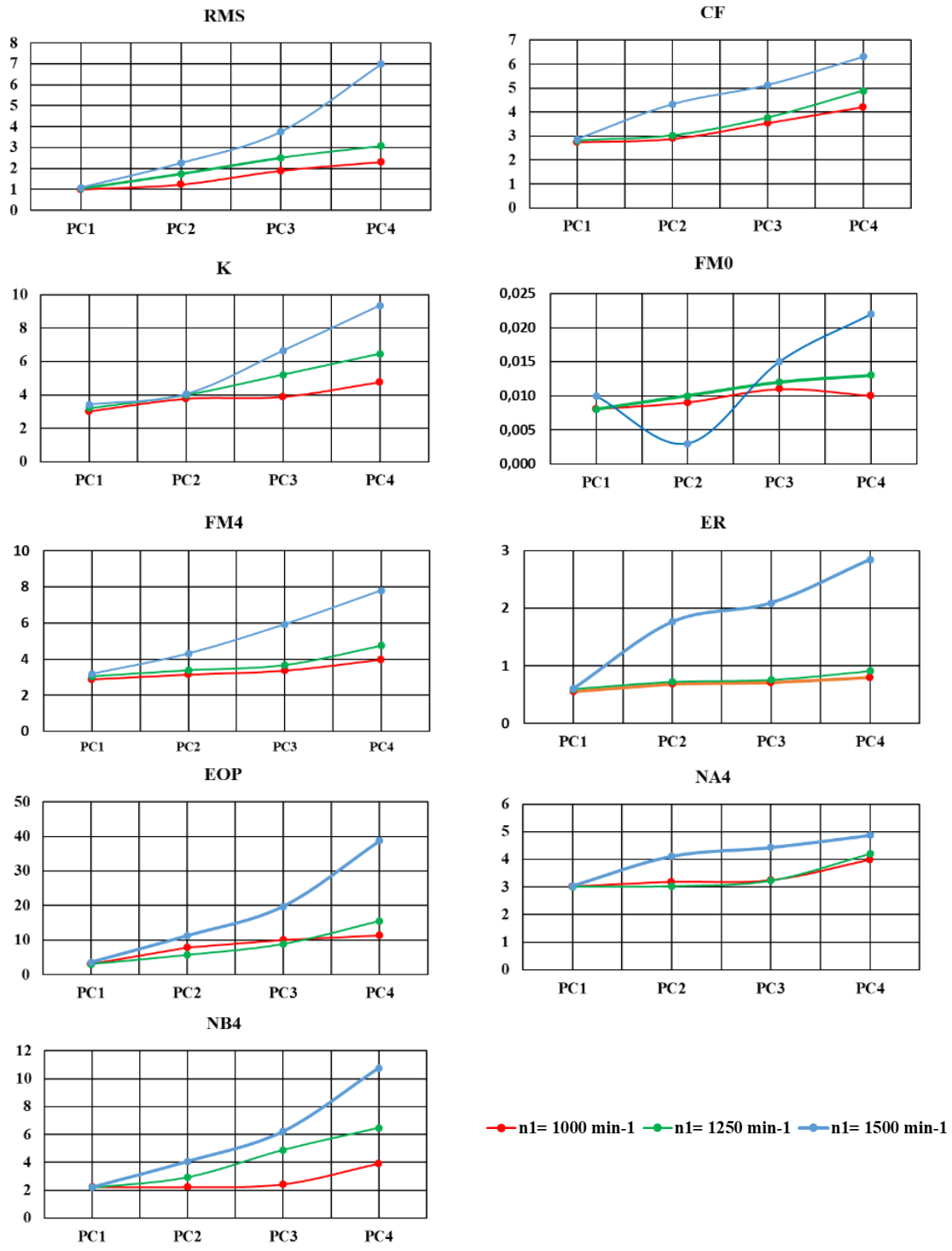

DOI: https://doi.org/10.14232/analecta.2022.1.34-41

Figure 3. Variation of CMI's for different input speeds and failure status

As one can observe, all the nine indicators are working well, displaying increased shapes with the growth of the speed, respectively of the severity of the pitting. If in the case of the input speeds of 1000 $min^{-1}$and 1250 min^{-1}, respectively, the increases of the nine investigated parameters are not spectacular, but still visible, with the aggravation of the pitting failure, this becomes obvious at the maximum speed (1500 min^{-1}) of the gearbox input shaft.

Regardless of speed, the most receptive parameters to gear failure were in descending order, EOP, RMS, NB4 and ER. In this sense, Fig. 4 provides a visual proof of this finding. At the minimum investigated speed, the least sensitive parameters proved to be FMO, NA4 and FM4, a characteristic that was maintained even at the maximum speed of the input shaft.

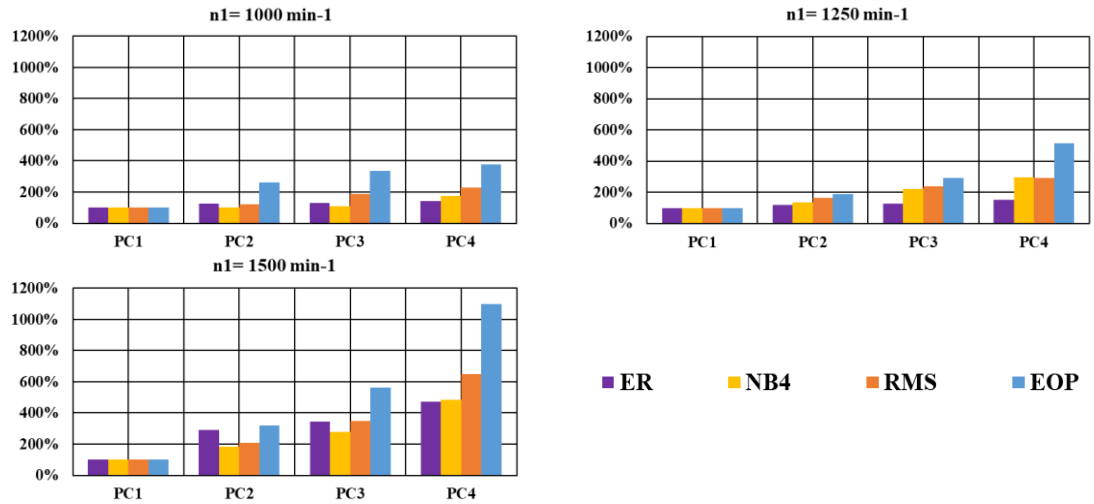

Figure 4. Percentage variation of the parameters with the highest sensitivity

Starting from these findings, we express the opinion that based on the previous analysed condition monitoring parameters extracted in time domain, it would be possible to classify the gear pitting stage, by involving machine-learning techniques. This capability will prove effective, especially in the case of fluctuating speed operating regimes, when frequency spectrum analysis is no longer applicable.

5. CONCLUSIONS

Gearboxes have wide application in different industries for speed and torque conversion. Inappropriate failure of the gearbox can be costly. Therefore, an early diagnosis of faults is very critical for their reliable operation.

In this study, experiments were performed for various gear pitting stages at three different input speeds. A comparative study of RMS, Crest Factor, Kurtosis, FM0, FM4, Energy ratio, Energy operator, NA4 and NB4 has been done for no, slight, mild and acute pitting of a pinion. This research highlights that all the indicators are responsive and sensitive to fault diagnosis, even at a low operating speed. Moreover, the experimental result indicates that CMI's describing the overall vibration level track the condition of the tested gearbox condition very well. Certain CMI provide not only information that something has happened in the gear transmission but they provide information about what has happened.

DOI: https://doi.org/10.14232/analecta.2022.1.34-41

Furthermore, the condition monitoring indicators may be involved, together with machine learning techniques, to classify the gear pitting status, in case of fluctuating speed operating regimes, where spectral analysis is more difficult to apply.
Additionally, these CMI's need to be also checked for fluctuating loading condition which is going to be the next goal in the area of non-stationary signals with non-constant operating circumstances. Our further research will be focussed on this topic.

REFERENCES

[1] Z. I. Korka, A. Bara, B. Clavac, L. Filip, Gear Pitting Assessment Using Vibration Signal Analysis, Romanian Journal of Acoustics and Vibration, 14 (1) (2017), pp. 44-49.
[2] K. Feng, W. A. Smith, R. B. Randall, H. Wu, Z. Peng, Vibration-based monitoring and prediction of surface profile change and pitting density in a spur gear wear process, Mechanical Systems and Signal Processing, 165 (2022), 108319.
[3] P. Kund, A. K. Darpe, M. S. Kulkarni, A correlation coefficient based vibration indicator for detecting natural pitting progression in spur gears, Mechanical Systems and Signal Processing, 129 (2019), pp. 741-763.
[4] S. Raadnui, Condition monitoring of worm gear wear and wear particle analysis of industrial worm gear sets, Wear, 476 (2021), 203687.
[5] R. B. Randall, W. A. Smith, P. Borghesani, Z. Peng, A new angle-domain cepstral method for generalised gear diagnostics under constant and variable speed operation, Mechanical Systems and Signal Processing, 178 (2022), 109313.
[6] P. Gandhi, N. Turk, R. Dahiya, Health monitoring of induction motors through embedded systems-simulation of broker rotor bar fault and abnormal gear teeth fault, Microprocessors and Microsystems, 76 (2020, 103077.
[7] H. Liu, S. D. Jaspreet, A time domain approach to diagnose gearbox fault based on measured vibration signals, Journal of Sound and Vibration, 333(7) (2014), pp. 2164-2180.
[8] V. Sharma, Gear fault detection based on instantaneous frequency estimation using variational mode decomposition and permutation entropy under real speed scenarios, Wind Energy, 24 (2021), pp. 246–259.
[9] J. Cai, X. Li, Gear fault diagnosis based on time–frequency domain de-noising using the generalized S transform, Journal of Vibration and Control, 24(15) (2018), pp. 3338-3347.
[10] X. Liu, H. Huang, J. Xiang, A personalized diagnosis method to detect faults in gears using numerical simulation and extreme learning machine, Knowledge-Based Systems, 195 (2020), 105653.
[11] Z. Y. He, H. D. Shao, X. Y. Zhang, J. S. Cheng, Y. Yang, Improved deep transfer auto-encoder for fault diagnosis of gearbox under variable working conditions with small training samples, IEEE Access 7 (2019), pp. 115368–115377.
[12] E. Bechhoefer, R. Li, D. He, Quantification of condition indicator performance on a split torque gearbox, Journal of Intelligent Manufacturing, 23 (2012), pp. 213-220.
[13] Z. I. Korka, Research on vibration reduction in operation of cylindrical gearboxes, PhD Thesis, "Eftimie Murgu" University of Resita, Romania, 2009.

DOI: https://doi.org/10.14232/analecta.2022.1.34-41